John Isotherm for the characterisation of microporous carbons: A comparative evaluation of adsorption phenomena

V Sivanandan Achari*,[1], Mercy Thomas, S Jayasree, A S Rajalakshmi, Raichel Mary Lopez & Bindia Ravindran

School of Environmental Studies

Cochin University of Science and Technology

Kochi 682 022 India

E-mail: vsachari@gmail.com / vsachari@cusat.ac.in

John *(J)* isotherm model stated as $\log\log P = C + n\log V$, for solid-gas equilibrium, is a unique contribution from India for the study of porous materials. These isotherms are generally characterised by different phases of adsorption marked by a sudden change in slope and sharp kinks in isotherm plots of loglog P versus log V. John isotherm is otherwise known as the phase change method. The isotherm model envisages the degree of porosity, by which the categorisation of porous materials could be done. The volume adsorbed, *V(J)* corresponding to saturation pressure P_s is taken as the limiting micropore volume (LMV) or John adsorption capacity. The adsorption behaviour of some known microporous carbons has been analysed using John isotherm. John isotherm along with five other isotherm models, Freundlich, Langmuir, D-R, BET and I plot methods are studied, constants and parameters are compared. There are three carbons, namely GC, its hydrogen treated form H2TGC and the nitric acid treated prodigy NITGC, whose isotherm data available is used to plot John isotherms to report the merits of the isotherm method. The results reveal that John isotherm model give excellent fit to the reported experimental data and provide precise information about the funcional mechanism of adsorption. The study aims to establish the application of John isotherm as a simple empirical isotherm model for characterising the microporosity of carbon materials over a wide range of concentration and relative pressure. The main purpose of this research paper is to reaffirm the application of John isotherm for its universal acceptance to study materials of microporous nature.

Keywords: Activated carbon, Adsorption, John isotherm, John-Sivanandan Achari equation, Microporous carbon, Adsorbability constant

John isotherm models[1,2] are used to express the adsorption phenomena exhibited by numerous porous materials. In general, empirical isotherm models conform to constants and parameters to determine the porosity and surface area of materials, rather effortlessly based on the adsorption[3-6] phenomena. Porous materials, microporous carbons and similar adsorbents undergo solid-gas or solid-liquid equilibrium adsorption process[2,7,8] under saturation conditions. Knowledge on porous structure of the material under investigation is inferred from the linear fit of an experimental adsorption isotherm model[9]. Thereby a comparison of different isotherms could be done for testing and finally a most suitable one is selected to describe a specific adsorption process[10-12]. This improves the reliability of isotherm evaluation. Mostly, pore volume, surface area and pore size distribution are used to evaluate the adsorption efficiency of materials. Freundlich model, Langmuir isotherm, Dubinin-Radushkevich (D-R) equation and Brunauer-Emmett-Teller (BET) method are frequently used for surface area determination of porous materials[13-17]. BET model is generally applied upto relative pressure range 0.05-0.3 based on the assumption that monolayer is being completed at this stage. Scatchard-type modified form of BET equation called, I plots[18,19] is used to estimate C parameter in the whole range of pressure $0 < p/p_0 < 1$. They are particularly used to characterise mesoporous materials having with extensive microporosity. Those materials attain monolayer at $p/p_0 < 0.3$ with an inversion point (I_{pt}) specific for each materials.

A change in the isotherm shape with respect to pore filling behaviour can be used as an analytical method for the determination of structural parameters of porous materials. In this regard, John isotherm[1,2] has many advantages for the structural characterisation of porous materials. John isotherm

regularly appeared earlier, only a few articles have been published during the last decade[2,7,11]. John isotherm model can be used to determine the adsorption capacity $V_m(J)$ (solid-gas) or $q_m(J)$ (solid-liquid) from equation (1) and (2). The agreement of John isotherm equation with (D-R) equation earlier verified by Nagpal and John[20]. John isotherm model can also be transformed into the Langmuir isotherm model[1,2]. John *et al.* (1985)[1] applied the BET method to determine the monolayer capacity and surface area from mixture adsorption. The applicability of Freundlich isotherm to determine adsorption capacity from some Type I isotherms and the significance of its constants was discussed[21]. This paper refers and reports a few cases where John isotherm model can be successfully used for the structural characterisation of microporous carbons using N_2/77K solid-gas isotherm. A study on adsorption behaviour of copper acetate over a wide range of concentration (1.0×10^{-8} - 1.0×10^{-1} mmol/g), where double fittings of Langmuir and Freundlich isotherm models were used[22] drawn special attention. This range of concentration is the common level of the contaminants in most water pollution studies. Numerous new forms of carbon materials are recently invented[23] that necessitate new isotherm models for testing and evaluation of their yet to be explored fundamental properties. The enumeration of the merits of already known isotherm models for the porosity and surface area evaluation of these new generation materials become essential particularly during their structural characterisation[24].

Experimental Section

Published data[1,2,22] have been identified to test John isotherm bears many of its significance. Study is based on microporous carbons, specific surface treatment procedures are applied and solid-gas and solid-liquid adsorption studies are systematically done to correlate the adsorption phenomenon. Farooq *et al.* (2009)[22] reported the experimental isotherms for the adsorption of nitrogen molecule at 77K and aqueous copper acetate solutions over a large range of linearity under varying concentrations, on three microporous carbon materials GC, H2TGC and NITGC. In the present study, John isotherm is modeled according to Equation (1) or (2) using this reported data[22]. BET surface area also published by these researchers, for carbons, from which the BET monolayer value, V_m *(BET)* could be calculated, using equation (19). This

is compared with the adsorption capacity V_m *(J)* obtained from John isotherm plotted according to Equation (1). Modified Freundlich (F), Langmuir (L), Dubinin–Radushkevich (D-R) isotherm models and *I* plots are taken further to evaluate the John isotherm model parameters (solid-gas). Equations (10), (11) and (16) are used to determine the characterisation energy E_0 kJnm/mol and mean pore width L_0 nm for Dubinin-Radushkevich and John isotherm models in an identical range of relative pressure and compared for microporous carbons.

John isotherm parameters for liquid phase adsorption are compared with the reported values[22] of Langmuir and Freundlich models. Error analysis is done using various statistical deviation functions[25,26]. Isotherm evaluation of the above microporous materials are done using models described here under.

John Isotherm model

John isotherm model[1] is stated as

$$\log \log P = C + n \log V \quad \text{(solid-gas)} \qquad ...(1)$$

where $P = p/p_0 \times 10^N$, N is an integer usually between 3 to 6 used so as to make the *logP* positive and *loglog P* is found.

Later the application of John isotherm model was extended to liquid phase adsorption[2, 27] is regarded as John-Sivanandan Achari (J-SA) isotherm equation.

John-Sivanandan Achari Isotherm Equation

$$\log \log C_e = C + n \log q_e \quad \text{(solid - liquid)} \qquad ... (2)$$

$$\log q_e = \frac{\log \log C_e - C}{n} \qquad ... (3)$$

Logarithm of monolayer capacity of any adsorbent is related to equation (3) where C and n are the intercept and slope respectively and plots are drawn accordingly. If there are instances where the equilibrium concentrations do not give a positive value in its *log* form, C_e is multiplied by an integer, such that $C_e = C_e \times 10^N$. Where *N* is an integer, so chosen that lowest *loglogC_e* of the data becomes positive[2]. The value of *logq_e* corresponding to the highest *loglogC_e* is taken as *log q_m(J)*, antilogarithm gives the monolayer capacity (LMV-Limiting Micropore Volume) for the isotherm with one

adsorption phase. More than one phase of adsorption exposed in the isotherm plot, reasonably justifies the dissimilarity become visible in the adsorption mechanism already proposed due to the heterogeneity of the porous surface.

John monolayer capacity, $V_m(J)$ or Limiting micropore volume (LMV)

On applying John isotherm using equation (1), to adsorption systems (solid-gas), a single straight line represents mono disperse porosity with a single type of adsorption mechanism for filling of micropores. The volume adsorbed corresponding to saturation pressure on the extrapolated straight line to the '*loglog P*' axis can be taken as the adsorption capacity $V_m(J)$. Sharp kinks are obtained by sudden changes in slope in the respective graphs to give different phases of adsorption, indicate the difference in the pore diffusion mechanism. The adsorbed volume $V_m(J)$ corresponding to the first kink is considered as the completion of John adsorption monolayer (*LMV*) for most microporous materials unless there are any molecular sieve effects, indicated by $V_{mse}(J)$. If any second phase is obtained near saturation, the first line connecting the lower experimental points, is extrapolated to *loglogP axis* (where $p/p_0 \approx 1.0$). In most cases, p/p_0 is multiplied with a factor 10^N such that $p/p_0 \times 10^N$ will be a positive integer, to enable the graphical simulation.

John mesopore volume $V_{me}(J)$

The John mesopore volume $V_{me}(J)$ is obtained by subtracting John monolayer volume $V_m(J)$ from John total adsorption capacity $V_T(J)$ for type II and IV isotherm. Another method used to predict the mesopore surface area by John is also known[28].

Categorisation of microporous carbon from the slope of John isotherm

The slope of the respective line graphs are given by equation (4).

$$n = \frac{\log \log P_s - \log \log P_1}{(\log V_s - \log V_1)} \quad ...(4)$$

Slope (*n*) referred as a measure of adsorbability or adsorption efficiency of the isotherm depends on V_s and V_1.

Equation (1) follows that

$$\log V_s = \frac{\log N - C}{n} \quad ...(5)$$

where C is the intercept and n the slope of the graph. $Log\ V_s$ obtained using (5) is compared to $logV_1$. When $V_1 \approx V_s$, the majority adsorption take place below the pressure P_1 and finer micropores at low pressure are filled. Micropores are small (d= ‹ 2.0 nm) and van der Waals forces from the walls of the pores overlap result in a very strong adsorption. If $V_1 \approx V_s$, slope '*n*' will be large with a narrow range of micropores containing large degree of finer microporosity. When $V_s > V_1$ lower pressures adsorption at P_1 is small and adsorption progress continuously with pressure results in small '*n*' indicates range of pore size is wide with small degree of finer microporosity. Hence '*n*' is used as an indicator of size, range and degree of microporosity[29].

Freundlich isotherm model

Freundlich isotherm model[30] describes heterogeneous non ideal adsorption on microporous materials. Freundlich equation could be deduced from John isotherm model[21]. Present study, applied the modified Freundlich equation (7), so that Freundlich and John isotherm model, obtain almost identical parameters accounting the heterogeneity of the carbon surface.

$$Q_e = K\ C_e^{1/m} \quad Or \quad V = K_F\ P^{1/m} \quad ...(6)$$

On taking logarithm it is transformed into a new form after properly rearranged, hereto referred as Modified Freundlich equation with slope *m* and intercept *m log K_F*

$$\log V = \log K + \frac{1}{m} \log P \quad ...(6.a)$$

$$\log P = m \log V - m \log K_F \quad ...(7)$$

where K_F (measure of adsorption capacity) and $1/m$ (measure of intensity of adsorption) are constants. John (1988)[21] showed that the constant '*m*' of Freundlich equation, is a function of '*n*', the absorbability constant of John's isotherm. These unique isotherm models are applied to the above reported[22] microporous materials. The Freundlich adsorption capacity $V_m(F)$ comparable to John adsorption capacity $V_m(J)$, is obtained by plotting *log P (*on y-axis) and *logV* (on x-axis), the antilogarithm of the highest adsorption point in the linear plot, at saturation pressure is taken[21].

Langmuir model

The Langmuir model[31] assumes the homogeneity in energy during adsorption on solid surfaces and no lateral interaction is expected between the adsorbed molecules. The well known linear form of expression (solid-gas) for the Langmuir model is given in equation (8).

$$\frac{P}{V} = \frac{1}{V_s b} + \frac{P}{V_s} \qquad \ldots (8)$$

where P is the pressure, V the gas volume adsorbed per unit weight of solid (cm^3/g) STP and V_s the saturation monolayer capacity, taken as the monolayer volume $V_m(L)$ per unit weight of solid (cm^3/g) STP and b is called the binding constant[32].

Dubinin-Radushkevich equation

The Dubinin-Radushkevich[33] (D-R) equation, regarded as a unique model for microporous materials can be expressed as

$$\log V = \log V_s - 2.303 \left(\frac{RT}{\beta E_0}\right)^2 \left[\log\left(\frac{p_0}{p}\right)^2\right] \ldots (9)$$

$$\log V_{ads} = \log V_0 - D_0 \left[\log(p_0/p)\right]^2 \qquad \ldots (9.a)$$

The plot of *logV* against *log $(p_0/p)^2$* is called the Dubinin-Radushkevich (D-R) isotherm plot. The micropore volume $V_{mic}(D-R)$ can be determined from the intercept of the D-R plot giving more thrust to the data for lower saturation pressure preferably upto $p/p_0 = 0.30$. The equation is mostly applied to type I microporous materials, as per IUPAC classification[34].

Characterisation energy E_0 kJ/mol is calculated from D-R plot using the formula

$$E_0 = \sqrt{\frac{2.303}{D_0} \frac{RT}{\beta}} \qquad \ldots (10)$$

where D_0 is the slope of *D-R* plot, R=0.008314 kJ/K/mol and β is the affinity coefficient taken 0.33 for N_2/77K. The mean pore width (L_0 nm) is found

$$L_0(nm) = \frac{10.8}{(E_0 - 11.4)} \qquad \ldots (11)$$

The complete identity of the isotherm equations of Dubinin and John for determination of the micropore volume and degree of microporosity of carbon was proved by Nagpal and John(1978)[20]. It was shown that slope 'D_0' of Dubinin equation, is related[20] to the parameters of John isotherm model n and N as given in equation (12)

$$D_0 = \frac{1.1}{n N^2} \qquad \ldots (12)$$

Also it was shown in the same reference[20],

$$D_0 = \frac{0.434 (2.303R)^2 T^2 K_1}{\beta^2} \qquad \ldots (13)$$

where K_1 is a constant related to differential molar work of adsorption. Equations (12) and (13) are identical and can be equated to each other.

But, the characterisation energy E_0 of D-R equation is related to its slope D_0

$$D_0 = \frac{2.303}{E_0^2} \left(\frac{RT}{\beta}\right)^2 \qquad \ldots (14)$$

Thereby equations (12) and (14) are equated, to connect the adsorption intensity 'n' of John isotherm model to find the characterisation energy.

$$\frac{1.1}{n N^2} = \frac{2.303}{E_0^2} \left(\frac{RT}{\beta}\right)^2 \qquad \ldots (15)$$

Or

$$E_{0(J)} (kJ/mol) = \frac{1.447 N R T \sqrt{n}}{\beta} \qquad \ldots (16)$$

BET Isotherm Equation

Brunauer, Emmett and Teller (BET)[17] proposed an isotherm equation for multilayer adsorption in 1938. The model gives suitable values of $V_m (BET)$, once the monolayer adsorption is completed on surfaces, which can be used to calculate the specific surface area *(SSA)* of microporous materials. The BET equation could be written as equations (17) and (18).

$$\frac{1}{V\left[\left(\frac{p_0}{p}\right) - 1\right]} = \frac{C-1}{V_m C} \left(\frac{p}{p_0}\right) + \frac{1}{V_m C} \cdot \qquad \ldots (17)$$

$$(\frac{p}{p_0}) / V [1 - (P/P_0)] = 1/CV_m + (C-1) (P/P_0) / C. V_m$$

$$... (18)$$

The plot of $(p/p_0)/V[1-(p/p_0)]$ versus (p/p_0) drawn in the adsorption range $0 < (p/p_0) < 0.30$ mostly conforms to a straight line, from which the constant $V_m(BET)$ the monolayer adsorbed quantity at saturation pressure p_s and C the BET constant are obtained. The method is based on the assumption that monolayer is completed in this ranges pressure. It has been rarely used unravel the behaviour of extending of microporosity in presence of other (wider) pores. Monolayer volume $V_m(BET)(cm^3/g)$ STP[18] of a porous material can be calculated using equation (20), if the material is having a reported $SSA_{(BET)}$ in m^2/g.

$$V_m \text{ (BET) (cm}^3/\text{g) STP} = \frac{SSA_{(BET)} \text{ (m}^2/\text{g)} \times 22414 \text{ (cm}^3/\text{mol)}}{6.022 \times 10^{23} \text{(molecules / mol)} \times 0.162 \times 10^{-18} \text{(m}^2/\text{ Nmolecule)}}$$

$$...(19)$$

This can be modified into

$$V_m \text{ (BET) (cm}^3/\text{g) STP} = \frac{SSA_{(BET)} \text{ (m}^2/\text{g)}}{4.356} ... (20)$$

Monolayer volume (cm^3/g) STP is converted to (ml/g), the liquid volume of N_2 at 77K by multiplying V_m using a factor 0.001547.

I plots

I plots[18] are created by modifying the BET isotherm to describe adsorption isotherm behaviour of porous materials with extensive microporosity.

$$\frac{V [1 - (P/P_0)]}{(P/P_0)} = C V_m - (C-1) V (1 - P/P_0)$$

$$...(21)$$

A plot of $\frac{V(1-P/P_0)}{(P/P_0)}$ versus $V(1-P/P_0)$ give an inversion point (I_{pt}). The $V_m(I)$ can be directly read from the x axis at the inversion point.[35]

Error Functions

The nonlinear form of John isotherm model[1] $logP=N(V/V_s)^n$ is linearised to equation (1) and evaluated, using five statistical deviation functions and two correlation coefficients[36,37]. For this purpose, the predicted value, $logV_{cal}$ is found from John isotherm model, using equation (22).

$$\log V_{cal} = \frac{(\log \log P - C)}{n}. \qquad ... (22)$$

Where C and n, are the slope and intercept of equation (1). It is then tested using five different error functions[25] such as sum of absolute errors (SABE), residual sum of squares (RSS), average relative error(ARE), a derivative of Marquardt's percent standard deviation (DMPSD), the hybrid fractional error function (HYBRID).The correlation coefficients $P(r)$ and $adj.r^2$ are determined using regression analysis.

A) *Sum of Absolute Errors (SABE)*

$$SABE = \sum_{j=1}^{q} \left| Q_{exp\,j} - Q_{cal\,j} \right| \qquad ...(23)$$

B) *Residual Sum of Squares (RSS)*

$$RSS = \sum_{j=1}^{q} (Q_{exp\,j} - Q_{cal\,j})^2 \qquad ...(24)$$

C) *Average Relative Error (ARE)*

$$ARE = \sum_{j=1}^{q} \left| \frac{Q_{exp\,j} - Q_{cal\,j}}{Q_{exp\,j}} \right| \qquad ...(25)$$

D) A Derivative of Marquardt's Percent Standard Deviation (DMPSD)

$$DMPSD = \sum_{j=1}^{q} (\frac{Q_{exp\,j} - Q_{cal\,j}}{Q_{exp\,j}})^2 \qquad ...(26)$$

E) The Hybrid Fractional Error Function (HYBRID)

$$HYBRID = \sum_{j=1}^{q} [\frac{(Q_{exp\,j} - Q_{cal\,j})^2}{Q_{exp\,j}}] \qquad ...(27)$$

where 'q' is the number of observations, $Q_{exp,\,j}$ and $Q_{cal,\,j}$, the experimental and model-calculated values respectively for observation j.

Correlation coefficient of Pearson, P(r)

Karl Pearson coefficient of correlation *P(r)* is applied in the John isotherm model for measuring the

degree of relationship between $logV$ (X parameter) and $loglogP$ (Y parameter). The goodness of fit or the extend of linearity, is calculated using equation (28), r near to +1, indicate total positive correlation and r = 0, pointing to no correlation.

$$P(r) = \frac{N(\sum XY)-(\sum X)(\sum Y)}{\sqrt{[N\sum X^2-(\sum X)^2][N\sum Y^2-(\sum Y)^2]}} \quad ...(28)$$

Adjusted r ^{2}(adj.r^2)

Model improvement of the linear correlation coefficient 'r^2' is done by adjusting the number of predictors in the model, value near to 'one', is considered as a measure of good fit of the data.

$$adj.r^2 = 1 - \frac{(q - 1)}{(q - p)} (1 - r^2) \quad ...(29)$$

where 'q' is the number of observations taken to fit 'p' parameters.

Results and Discussion

John isotherm model, $loglogP = C + n\ logV$ is derived from Polyani's potential theory and had been applied for the study of porous materials[1,2,38]. It is possible to categorise and classify the microporous carbon from the shape of the John isotherm[29]. In this original paper by John *et al.*(1989)[29] the categorisation of microporous material is done based on nine different types of isotherm features. They were successfully analysed to account the different phases of adsorption and thereby explained the significance of the adsorption mechanism occurs on the material surface. The table of categorisation of microporous carbon from the shape of isotherm and the corresponding figures are well known[2]. The John adsorption capacity *V(J)* is obtained by taking the volume adsorbed (V_s) corresponding to the saturation pressure(P_s), the antilog of *logV$_s$*, is taken as the total pore volume $V_T(J)$ corresponding to saturation *loglogP$_s$*.

Surface modifications of porous materials through chemical and heat treatment leads to changes in porosity and pore dimensions. Accordingly, adsorption occurs through a series of phase change phenomena. John isotherm[2,29,39] suggests that adsorption process on porous materials include micropore filling first, followed by sub monolayer filling, then monolayer completion, mesopore filling(narrow) and mesopore filling (wide) and then the ultimate saturation. In type II porous materials, micropore filling in first phase is followed by mesopore filling in the second phase. Type IV isotherm follows micropore filling in phase I, mesopore filling in phase II, capillary condensation in phase III form hysteresis loop and ultimately free liquid formation at saturation.

The reported work[22] is based on coconut shell based three carbons namely GC, its hydrogen treated, H2TGC, heated at 950^0C and another nitric acid oxidised form NITGC, employed for the adsorption study using copper acetate solutions for a wide range of concentrations (1.0×10^{-8}- 1.0×10^{-1} mmol/g). Carbons on further heating/surface treatment, porosity and surface area as well as nature and content of surface complexes are changed. These researchers[22] reported the BET monolayer and Boehm titration data of all three carbons for comparisons.

H_2 treatment of the GC enhanced the surface area (SA) from (1560±30) to (1630±30) m^2/g. But nitric acid treatment reduced it to (1330±30) m^2/g. Boehm titre value for phenolic surface groups have been GC: (0.09±0.01), H2TGC: (0.03±0.01) and NITGC: (3.3±0.1) mmol/g respectively. These indicate marked changes in the surface chemistry and porosity of the carbon. A sum of two Langmuir isotherms was applied for the whole range of concentration of Cu^{2+} ions adsorbed by these carbons during adsorption in liquid phase. Distinct changes are observed in the plots with respect to John isotherm, in relation to surface treatments provided. These features together with the support of other isotherm models, give significant information on the material behaviour. A combination of isotherm model equations applied in the referred paper[22]. Whereas, in this study a single isotherm equation is fitted for both lower and higher concentrations of the AAS data obtained for Cu^{2+} ions adsorption. This has been one of the advantages observed for the John isotherm model applied in this extensive study presented.

The John isotherm plots of carbon GC, presented as Fig. 1 based on N_2 uptake data provide three distinct phase changes. Phase I ($p/p_0 \approx 1.5\times10^{-6}$to 8.9×10^{-6}) region of molecular sieve effects (mse) extends upto the onset/ beginning of finer micropore filling completed at $V_f(J)$in phase II. Then branches off to a straight line in the graph, where the monolayer completion occurs in micropores at

saturation pressure in phase III ($p/p_0 \approx 7.6\times10^{-4}$ - 8.4×10^{-1}). The John isotherm plots of carbons and their respective Freundlich and *I* plots are shown in Fig. 2 and Fig. 3.

This suggests three different mechanisms are operating from lower to higher relative pressure range. Phase I of carbon (GC) is comparable to John type behaviour for microporous category 7, describes isotherm has an upward deviation at very low pressure range[2].Because some pores of adsorbents are smaller than adsorbate molecules. At extremely low pressure range, the straight line has an upward deviation, indicates, some pores of the acid-washed GC are not access to nonpolar N_2 gas, due to the presence of surface functional groups, since (D < d) [40]. Mostly basic pyrones like groups (0.74 ± 0.01) mmol/g, acidic surface groups, like phenolic (0.09 ± 0.01), carboxylic (0.00 ± 0.01) and lactonic (0.07 ± 0.01) mmol/g are present.

Hence molecular sieve effects (mse), cause lower adsorption to take place in phase I (GC),equal to an adsorption capacity of 97.7 cm^3/g (Table 1). The slope of the graph '*n*' (John adsorbability constant) is found to be 0.21. This indicates, the adsorption potential is less in this region. Contribution by finer pores is less for microporosity of the material.

The end of this mechanism is indicated at the cut off value of adsorbed volume, corresponding to the $logV_{mse}$(J) indicated by a sharp kink in phase I (GC). Thus in phase I (GC) the active adsorption is restricted imposing molecular sieve effects.

Phase II (GC) of John isotherm (p/p_0= 8.9×10^{-6} to 7.6×10^{-4}) indicates the presence of micropores, typical for microporous carbon similar to John's category[2] Type 2. Here, two lines connect all the experimental points indicate bidisperse porosity – the finer micropores and the coarser (wider micro) pores. John adsorbability constant *n* is noted as 0.70, in this region adsorption is more prominent.

At this ranges, adsorbate is accessible into the internal pores of the graphene layers (D = d or d < D < 2d)[40] evidenced by a distinct phase II(GC)with slope having value n(GC) 0.7 and phase III (GC) with adsorbability constant *n* equal to 1.06, for saturation (D = 2d or D > 2d)[40]. The contribution of wider micropores V_c(*J*) is obtained by subtracting [V_{mse}(*J*)+V_f(*J*)] of GC from V_m(*J*)GC, observed as 185.3 cm^3/g (Table 1), with adsorbability constant *n* equal to 1.06.

Figure 4 is the John isotherm plot of H2TGC, obtained by treating GC[22]with *5% H_2 at 950^0C.*
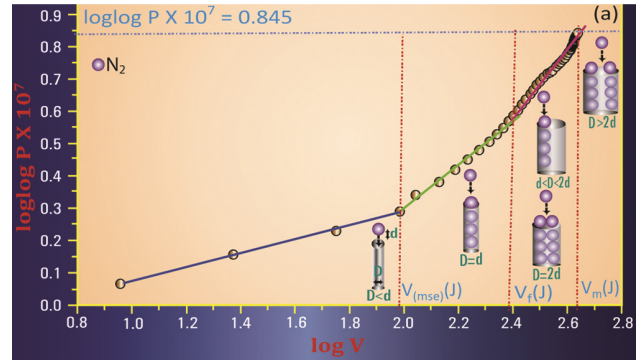
Fig.1 — John isotherm plot for N_2 at 77K for microporous carbon (a) GC using equation *loglogP=C+n logV*
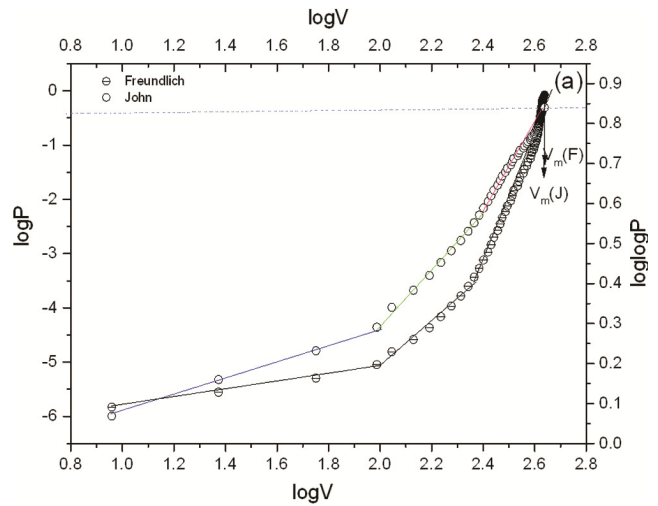
Fig. 2 — Freundlich isotherm for N_2 at 77K for microporous carbon (a) GC using equation *logP=mlogV-mlogK_F* along John isotherm
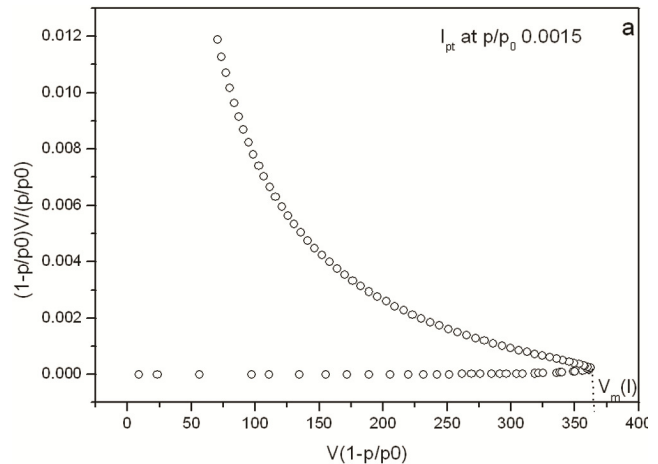
Fig. 3 — I plot for N_2 adsorption at 77K using equation $\dfrac{V(1-P/P_0)}{(P/P_0)} = CV_m - (C-1)V(1-P/P_0)$ for micro porous carbon (a)GC

Isotherm conforms to distinct phases- phase I (*H2TGC*) for a range of (p/p₀≈5.1×10^{-6} - 1.7×10^{-4}) represented by the first phase of straight line graph. Phase II (*H2TGC*) – branches off to two straight lines (phases) at the upper portion having a very short phase at saturation (p/p₀ ≈ 7.3×10^{-2} - 9.8×10^{-1}).

At phase I *(H2TGC)* substantial adsorption could be seen [$V_f(J)H2TGC$ 208.9 cm³/g, *n(H2TGC)=0.57*] compared to phase I of GC [$V_f(J)GC$ *97.7cm³/g,n₁(GC)0.21*]. This indicates, less prominence of molecular sieve effects and more accessibility (adsorption) of N_2 into porous structure of H2TGC. Means the changes in surface chemistry brought significant structural changes in the isotherm features. The hydrogen treatment cleaned up the surface of GC, free of carboxylic and lactonic surface functional groups. Phenolic and basic groups are preferentially removed from the surface, as it is evidenced by the Boehm titration data by the researchers[22]. In John isotherm model this is evidenced by a high slope (adsorbability constant) n_2=0.57(H2TGC) for strong interaction of N_2 with carbon micropores. Edges of graphene sheets are free and active to give way to N_2 molecules. This caused more adsorption to take place in micropores in phase I (H2TGC). Moreover, John *et al*. (1980)[41] reported that different degrees of activation done for the same adsorbent, can give different isotherm parameters particularly, on applying the same isotherm equation, for microporous materials. H2TGC, due to its activation at 950°C lead to an increase of porosity resulted in a high adsorption capacity in phase I (H2TGC).This is indicated by a comparatively steep isotherm feature with a sharp kink.

The BET surface area (reported)[22] for the *H2TGC* are also high. In the upper strata, the straight line in phase II (H2TGC) forms a small swing, with experimental points. This indicate the persistence of bidisperse porosity-the micro and coarser micropores. The original N_2/77K isotherm of reported carbons belong to type I of IUPAC[34] classification. Hence, they are categorised as micro porous materials only. Adsorption on H2TGC is influenced by the presence of very few basic surface functional groups (0.61±0.01mmol/g). Since enough acidic functional groups are not present on the surfaces, restriction to adsorption is minimum. In phase II (H2TGC), adsorption occurs into wide micropores as observed by earlier researchers[42] due to van der Waals dispersion and repulsion forces.
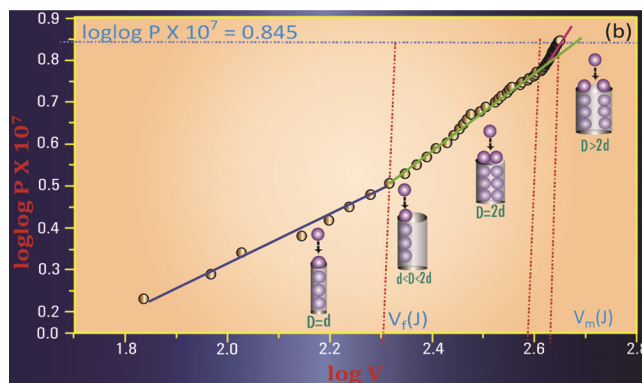
Fig. 4 — John isotherm plot for N_2 at 77K for micro porous carbon (b) H2TGC using equation $loglogP=C+nlogV$.
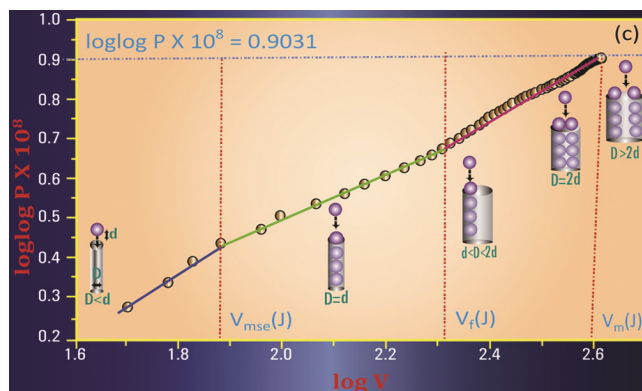
Fig. 5 — John isotherm plot for N_2 at 77K for microporous carbon (c) NITGC using equation $loglogP=C+nlogV$.

John isotherm plots for oxidised form of carbon NITGC is nitric acid oxidised form of GC whose surface has many active groups are given in Fig. 5. The HNO_3 acid treatment destabilised all the basic functional groups, only 0.02±0.01 mmol/g exists. Nevertheless, it created more acidic surface functional groups, phenols (3.3±0.1), lactones (2.2±0.1), carboxyl (1.3±0.1) mmol/g, on the surface of NITGC.

John isotherm model conform to three distinct phases during N_2 adsorption in this carbon with adsorption capacity $V_m(J)$ 416.9 cm³/g with respect to the saturation pressure p_s at ($loglogP$ ≈ 0.903).The successive surface treatment changed the surface heterogeneity with tunable features evident from (the measured adsorption capacity $V_{mse}(J)NITGC$ 75.9 cm³/g) phase I (NITGC) due to increased molecular sieve effects.This phase may also be influenced by the generation of extra acidic surface functional groups.This is directly observed with distinct phase changes in the John isotherm plots.The John isotherm adsorbed quantities (cm³/g) STP obtained from the graphs are summarised in Table 1.

Table 1 — John isotherm adsorbed amounts (cm^3/g) STP of nitrogen at *77 K* on GC, H2TGC and NITGC

carbon sample	From John isotherm graph			John adsorption capacity (cm^3/g)STP		
	$logV_{mse}(J)$	$logV_f(J)$	$logV_m(J)$	$V_{mse}(J)$	$V_f(J)$	$V_m(J)$
GC	1.99	2.4	2.64	97.7	153.5	436.5
H2TGC	-	2.32	2.65	-	208.9	446.7
NITGC	1.88	2.32	2.62	75.9	133.0	416.9

Table 2 — Characterisation energy E_0 KJ/mol and mean pore width L_0 nm of D-R and John isotherm

Carbons	p/p$_0$ range	Slope (D-R)	$E_{0(D-R)}$ kJ/mol	$L_{0(D-R)}$nm	Slope n(J)	N (J)	$E_{0(J)}$ KJ/mol	$L_{0(J)}$ nm
GC	1.6×10^{-5}- 3.0×10^{-1}	-0.023	19.41	1.35	0.881	7	18.44	1.53
H2TGC	5.1×10^{-6}- 3.0×10^{-1}	-0.025	18.50	1.51	0.790	7	17.46	1.8
NITGC	7.6×10^{-7}-3.0×10^{-1}	-0.023	19.25	1.38	0.666	8	18.32	1.56

Dubinin – Radushkevich (D-R) Isotherm plots and Characterisation Energy (E_0)

The D-R plots of the microporous carbons are drawn for comparing the results with John isotherm constants and that of (a) GC is shown in Fig. 6 .

The characterisation energy E_0 kJ/mol and mean pore width L_0 nm of carbons are determined for both Dubinin-Radushkevich (D-R) model and John isotherm model using respective equations (Table 2). The D-R plot of microporous carbons (b) H2TGC and (c) NITGC are also drawn and constants are evaluated. E_0 kJ/mol and L_0 nm have comparable values for Dubinin - Radushkevich (D-R) and John isotherm models considered for an identical range of relative pressure (p/p$_0$) < 0.30. Agreement of L_0 (D-R) and L_0 (J) evaluated through equations (10), (11) and (16) reveals both isotherms are most valuable for the structural characterisation of microporosity of materials. Also it indicates that H$_2$ treatment of GC to yield H2TGC lead to more activation with a comparatively large L_0 nm equal to L_0 (D-R) 1.51nm or L_0 (J) 1.8nm. Pore volume values of carbons are shown in Fig. 7.

Regression and Error function analysis

John isotherm model applied to GC, H2TGC and NITGC of N$_2$/77K show the best of its performance, evident from the adsorption isotherms (Table 3). Also from the values obtained for all the five error functions SABE, RSS, ARE, DMPSD and HYBRID adopted for the present study (Table 4). The coefficients of the carbons, for $P(r)$ and *adj.r^2* are near to 1.0, in all the three phases, implies excellent goodness of fit for John isotherm model.

It is proved as an appropriate model to interpret the behaviour of these data sets. The results of regression and error function analysis done for the John isotherm model are presented in Table 4. The slope *n (GC)* show a very small value of 0.21 at phase I of GC
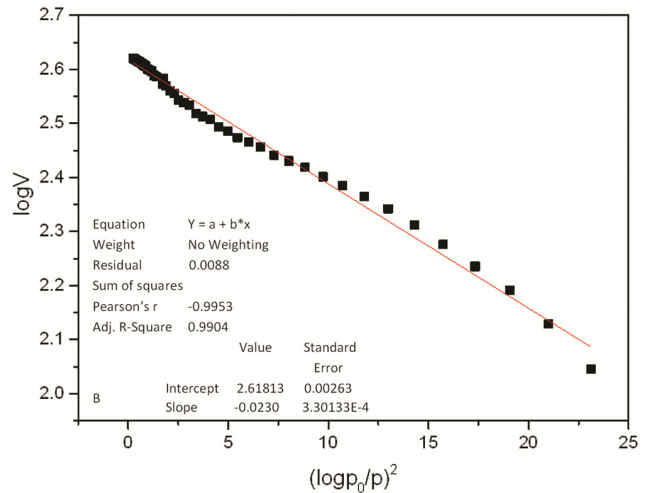
Fig. 6 — D-R plot of N$_2$ adsorption at 77K with linear fitting for microporous carbon (a)GC using equation $\log V_{ads} = \log V_0 - D_0 [\log (p_0 / p)]^2$
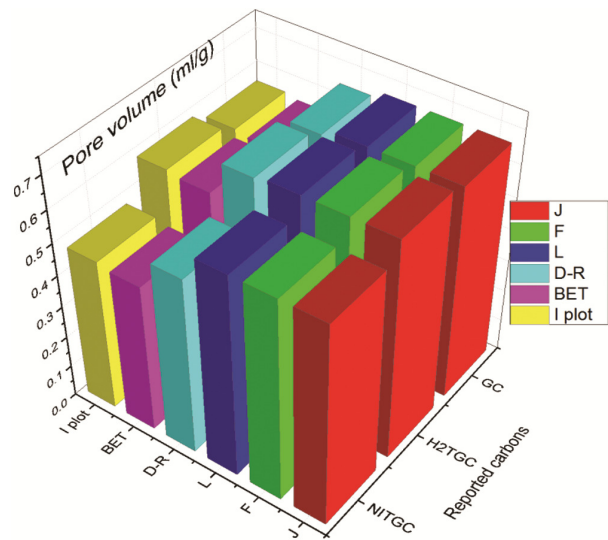
Fig.7 — Pore volumes obtained for John(J)/Modified Freundlich (F)/Langmuir (L)/D-R/BET/I plot isotherm models for the adsorption of N$_2$ at 77K for micro porous carbons.

Table 3 — Pore volumes obtained for John $V_m(J)$/ Modified Freundlich $V_m(F)$ / Langmuir $V_m(L)$/ DR $V_{mic}(DR)$ /BET $V_m(BET)$/ I plots$V_{mic}(I)$for the adsorption of N_2 at 77K for carbons ; GC, H2TGC and NITGC

Microporous carbons	$V_m(J)$ (cm^3/g)/ml/g	$V_m(F)$ (cm^3/g) /ml/g	$V_m(L)$ (cm^3/g) /ml/g	$V_{mic}(DR)$ (cm^3/g) /ml/g	$V_m(BET)$ from equation(20) (cm^3/g) /ml/g	I plot $V_{mic}(I)$ (cm^3/g) /ml/g
GC	436.5(0.67)	436.5(0.67)	431.0(0.67)	416.9(0.65)	358.13[*] (0.55)	364.4[**](0.56)
H2TGC	446.7(0.69)	446.7(0.69)	446.4(0.69)	436.5(0.68)	374.2[#] (0.58)	380.9[#](0.59)
NITGC	416.9(0.64)	416.9(0.64)	414.9(0.64)	363.1(0.56)	305.33[*#] (0.47)	312.7[**#](0.48)

[*]$(SA_{BET}1560)$,[#]$(SA_{BET}1630)$,[*#]$(SA_{BET}1330)$ and ([**]I_{pt} at p/p0=0.0015), ([#]I_{pt} at p/p0=0.0825), ([**#]I_{pt} atp/p0=0.0928).

Table 4 — Regression parameters and error functions of isotherm plots of N_2/ 77K for carbons GC, H2TGC and NITGC using equation $loglogP=C+n\ logV$

Adsorbent	Regression	John isotherm model		
		Phase I	Phase II	Phase III
	p/p0	1.5×10^{-6} - 8.99×10^{-6}	8.9×10^{-6} - 7.6×10^{-4}	7.6×10^{-4} - 8.4×10^{-1}
GC	Slope (n)	0.21	0.70	1.06
	Intercept (c)	-0.14	-1.09	-1.95
	P(r)	0.99	0.99	0.99
	adj.r^2	0.99	0.99	0.98
	SABE	5.1×10^{-3}	1.1×10^{-4}	2.8×10^{-3}
	RSS	1.1×10^{-3}	6.5×10^{-4}	5.5×10^{-3}
	ARE	3.1×10^{-3}	8.8×10^{-5}	1.15×10^{-3}
	DMPSD	3.8×10^{-4}	2.72×10^{-4}	7.38×10^{-4}
	HYBRID	6.4×10^{-4}	6.1×10^{-4}	1.92×10^{-3}
	p/p0	5.1×10^{-6} - 1.7×10^{-4}	1.7×10^{-4} –7.3×10^{-2}	8.2×10^{-2} –9.8×10^{-1}
H2TGC	Slope (n)	0.57	0.92	2.3
	Intercept (c)	-0.82	-1.62	-5.26
	P(r)	0.99	0.99	0.99
	adj.r^2	0.988	0.99	0.99
	SABE	1.25×10^{-5}	2.23×10^{-6}	5.25×10^{-4}
	RSS	6.50×10^{-4}	8.0×10^{-4}	2.30×10^{-4}
	ARE	1.85×10^{-4}	3.99×10^{-5}	2.0×10^{-4}
	DMPSD	4.5×10^{-4}	1.54×10^{-4}	6.22×10^{-6}
	HYBRID	9.4×10^{-4}	3.83×10^{-4}	1.64×10^{-5}
	p/p0	7.6×10^{-7} –5.1×10^{-6}	5.1×10^{-6}-5.3×10^{-4}	5.3×10^{-4}-9.9×10^{-1}
NITGC	slope	0.89	0.56	0.72
	intercept	-1.24	-0.62	-0.97
	P(r)	0.99	0.99	0.99
	adj.r^2	0.99	0.99	0.99
	SABE	4.54×10^{-6}	5.01×10^{-5}	6.7×10^{-4}
	RSS	4.0×10^{-5}	1.8×10^{-4}	1.5×10^{-3}
	ARE	5.7×10^{-6}	6.1×10^{-5}	3.2×10^{-4}
	DMPSD	1.6×10^{-5}	1.3×10^{-4}	4.5×10^{-4}
	HYBRID	2.8×10^{-5}	2.7×10^{-4}	1.1×10^{-3}

(p/p0 = 1.5×10^{-6}- 8.99×10^{-6}). The data at the region of saturation deviate prominently from the experimental line has *n (GC)* 1.06 is regarded as a saturation phase III of type I isotherm, because of filling at wider micro (coarser) pores. Phase I is common in several microporous systems where isotherm has an upward deviation at very low pressure range. The isotherm is represented by a steep line with shape of C as well as a sharp kink, because 'some of the pores are smaller than adsorbate molecules', (D < d) [40] due to activated

diffusion and molecular sieve effects to occur at low pressures[2].

The whole experimental points conform only to a single straight line for all the three carbons in the Langmuir model; assumes a homogeneous surface. But actually the carbon surface is heterogeneous as is evident from John (Figs 1, 4 and 5), Freundlich (Fig. 2) and I plots (Fig. 3). Dubinin-Radushkevich model give RSS value of 0.01, whereas modified Freundlich model give RSS value of (0.003) on

analysing the data for a range of $p/p_0 \approx 1.48 \times 10^{-6}$ - 9.00×10^{-6}. These are higher than that observed on applying to John isotherm plots. BET model is limited in usage upto relative pressure 0.3, and I plots showed distinct deviation at $I_{(pt)}$ located near to $p/p_0 = 0.0015$, reveals that the material is microporous.

On modification of GC by H_2 treatment the surface is made free of any acidic functional groups. The range of microporosity is increased in phase1 (H2TGC) indicated by the adsorbability n_1 is 0.122. The second phase II has also marked change indicating high adsorption effeciency n_2 (0.57).The highest slope, ($n_3 = 2.3$) is obtained for Phase III (H2TGC) implies the high ranges of porosity on this treated carbon. RSS value of Langmuir model is 8.7×10^{-9} relatively lower, for H2TGC. Comparatively higher RSS (0.03) is obtained for D-R model.Whereas, John isotherm model is prevailing with least RSS in all the three phases.

Residual plots of John isotherm model for the three microporous materials are presented in Fig. 8. They show clean patterns that reveal the nature of the dataset is nonlinear. The deviation of pore volumes (ml/g) of other isotherm with respect to john isotherm is given in Fig. 9.

Monolayer volume or Limiting Micropore Volume (LMV) of John isotherm model $V_m(J)$ and *further* comparison using percentage of deviation on applying other isotherm models are presented in Table 3 and Table 5. John (J), Modified Freundlich (F) and Langmuir(L) isotherm models offer almost identical values of monolayer volumes for the three carbons GC, H2TGC and NITGC in the present study. Deviation of John isotherm model with BET and I plot methods need more studies regarding interfering factors particularly for the carbon NITGC having more oxygen surface complexes.

In all cases of Langmuir isotherm applied, any factors mentioned in the above discussion are accessible. But its adsorption conforms to a more generally accepted homogeneous monolayer, common to a Type I (IUPAC)[34] isotherms characterised by its long horizontal plateau. John isotherm give excellent inferences regarding heterogeneous nature of the tested carbon materials whose surface is having with distinct bidisperse microporosity. In this study with respect to solid-gas equilibria using modified Freundlich and Langmuir, it is once again verified. John isotherm can be transformed to Langmuir and Freundlich isotherms for the determination of structural parameters[2,21].
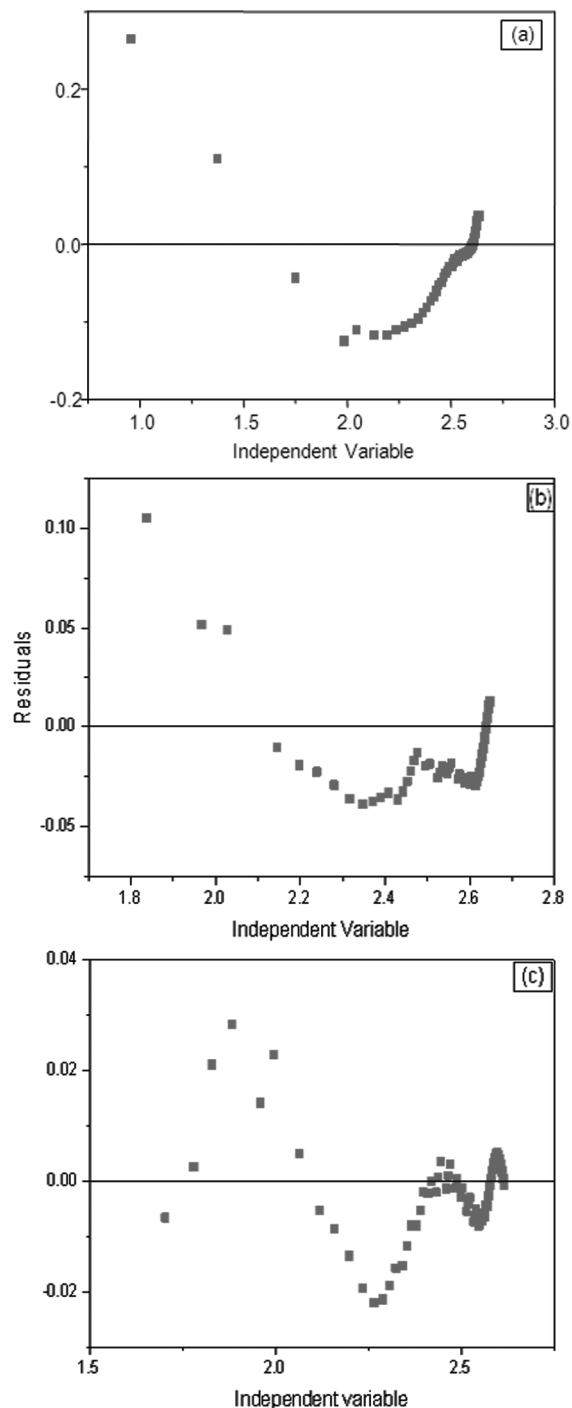
Fig. 8 — Residual plot of microporous carbon (a) GC; (b) H2TGC and (c) NITGC with respect to John isotherm model.

Application of John-Sivanandan Achari (J-SA) model to solid-liquid adsorption equilibrium

The published results of authors[22,43] are further subjected to isotherm analysis by the new method for liquid phase adsorption of GC, H2TGC and NITGC using copper acetate solution. The interaction of

copper acetate on microporous carbon surface is decided by the nature of surface structures of complexes, pore selectivity and acidity of the liquid medium. On applying John –Sivanandan Achari (J-SA) isotherm model[2,27] the extended form of John isotherm for liquid phase for the same data, distinct features can be seen in the graphs. Figure 10 indicates
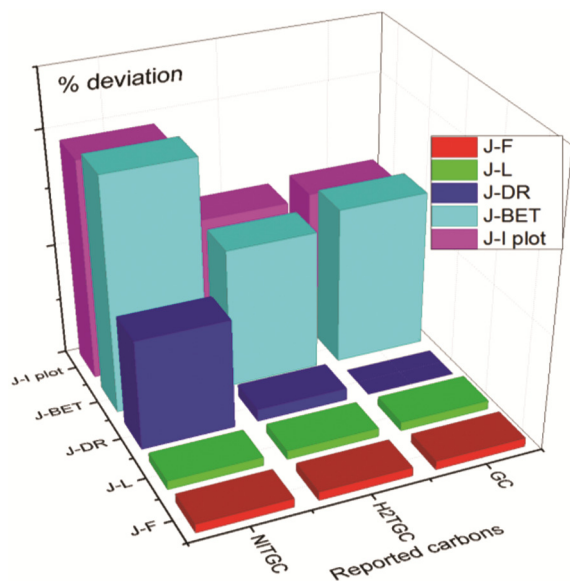
Fig. 9 — Percentage deviation of pore volumes (ml/g) of isotherm models with respect to John isotherm model.
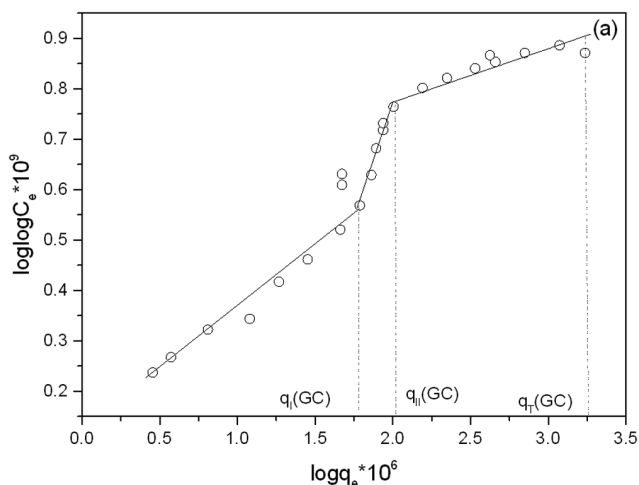
Fig. 10 — John-Sivanandan Achari (J-SA) isotherm plots for the adsorption of copper acetate on microporous carbon (a) GC using equation $loglogC_e=C+nlog\ q_e$.

the John –Sivanandan Achari (J-SA) isotherm plot of carbon GC for copper acetate adsorption. Isotherm has three distinct phases marked by kinks or distinct lines for phase change. Low concentration adsorption given in the phase I is generally attributed to the presence of surface functional groups[22]. The adsorption mechanism is interpreted distinctly based on phases appeared in the isotherm plot.

The irregular, randomly cross linked stacks of flat aromatic sheets on carbon matrix, posses heteroatoms with lower energy for valence orbitals. This give partial negative charge to them and thereby a partial positive charge will be delocalised over all the carbon atoms of the graphene layer. The electrostatic repulsive interactions of positively charged Cu^{2+} ions (a borderline acid as per HSAB concept[44]) with carbon surface are not profound in this phase, under the experimental conditions. GC contains both acidic and basic surface functional groups revealed through Boehm results[22] discussed earlier. Acidic surface groups exchange cations while basic surface groups exchange anions. Adsorption occurs at these surface functional group sites, originally present or incorporated at the edge of the aromatic sheet or in its microtexture[44] by ion exchange process. Adsorption contribution to phase I (GC) is found 0.06 mmol/g very near to the reported Boehm titration result (0.09 mmol/g) whereas the reported value for Langmuir no.1 adsorption is (0.08 mmol/g)[22]. The low slope n(GC) 0.24, indicates comparatively low intensity of adsorption[20] interaction.

Presence of a sharp kink obtained at the end of phase I(GC) (C_e= 5.1×10^{-6}) points to the change in adsorption mechanism and now the binding sites are accessible Cu^{2+} ions so as to evolve out as phase II indicated by adsorbability constant, the slope value n_2 for carbon GC is 0.45. In phase II (GC), adsorption may occur in the edges of graphene layers. If the pH of the solution is higher than the pH of zero charge (pH_{zpc}), the surface groups are ionised, and activated carbon is negatively charged[44]. This allows the trapping of Cu^{2+} ions in a strong electrostatic field, might have the reason for the increase in slope value for this adsorption phase. Another possibility is that

Table 5 — Percentage of deviation of pore volumes $V_m(ml/g)$ between John and respective isotherm models.

Carbons	J -F	J-L	J-(D-R)	J-BET	J –I plot
	$V(J_J)-V(F)/V(J)\times100$	$V(J)-V(L)/V(J)\times100$	$V(J)-V(DR)/V(J)\times100$	$V(J)-V(BET)/V(J)\times100$	$V(J)-V(I)/V(J)\times100$
GC	-	-	0.03	17.9	16.4
H2TGC	-	-	1.4	15.9	15.9
NITGC	-	-	12.5	26.6	25

the sp[2] hybridised hexagonal graphene layers act as Lewis base centres for protonation. However, competitive adsorption between H^+ and Cu^{2+} ions leads to lower surface coverage (0.04 mmol/g) for the latter (Table 6).

Again, a sharp kink is observed at (C_e=6.5×10^{-4}) indicates the change in mechanism of adsorption. This marks the creation of the phase III (GC), at high concentration. Generally, the third phase of John isotherm is due to capillary condensation for solid-gas equilibria. Moreover, the adsorption capacity during phase III (GC) is found to be (1.66 mmol/g), the highest adsorption noted among three phases (obtained by subtracting phase I and II adsorption from total adsorption capacity). But with a weak adsorption interaction indicated by a less adsorbability constant (n_3) value of 0.090 out of the three phases observed for this carbon. Microporous surface is accessible for Cu^{2+} ions in the selected concentration ranges substantially for adsorption interaction leads to Phase III (GC).

The possible and viable mechanism is explained on the basis of percentage of Cu^{2+} adsorption in each phase with respect to the total metal ion adsorption and based on adsorbability constant 'n_3' for phase III (GC). Only 3.4% of the total adsorption take place during phase I, 2.3% occur in phase II(GC) and 94.3% major proportion of Cu^{2+} ion adsorption occurs during the phase III(GC) as revealed in Fig. 11. This indicates the extensive interactions occurring in phase III (GC). But mostly of weaker π bond interactions indicated by a small adsorbability constant 'n_3' value of 0.090. High Cu^{2+} concentration cause more adsorption sites being occupied by them through ion exchange. Moreover, the hydrolysis products $Cu(OH)^+$ and $Cu(OH)_2$ present[45] in large quantities, are adsorbed through hydrogen bonding. Cu^{2+},

$Cu(OH)^+$ and $Cu(OH)_2$ may occupy the wide micropores, indicated on the GC leading to quasi capillary condensation[42] indicated by the phase III of John-Sivanandan Achari isotherm model. In phase III of GC the acetate ions formed may interact with the dense and delocalised pi-electron (aromatic) centres on carbon. Thereby bonding and antibonding molecular orbital created extensively throughout the graphene layers. The hydrolysis products of copper acetate support the major adsorption percentage of
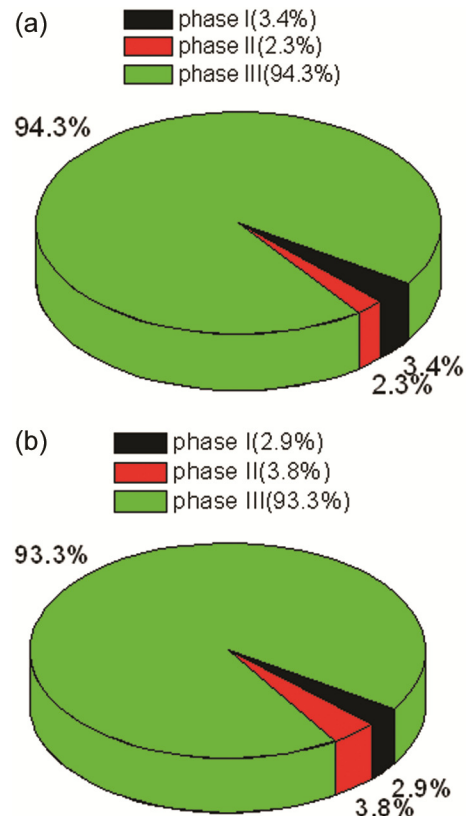
Fig. 11 — Percentage of phase wise adsorption of copper acetate with respect to its total adsorption on microporous carbon (a) GC (b) H2TGC

Table 6 — Adsorbed quantity (mmol/g) for John-Sivanandan Achari (J-SA)/ Langmuir (L)/ Freundlich (F) models of Cu^{2+} ions on micro porous carbons.

Carbons	John-Sivanandan Achari isotherm parameters						Reported values (mmol/g)[22]		
	Log value from graph			Adsorbed quantity q (mmol/g), Slope (n) /Measure of adsorbability (Phase wise)			Langmuir no:1	Langmuir no:2	Freundlich
	Phase I	II	III	q_I	q_{II}	*q_T (J-SA)			
GC	1.78	2.01	3.25	0.06 (n_1=0.24)	0.04 (n_2=0.45)	1.76 (n_3=0.09)	0.08±0.01	2.1±0.2	-
									-
H2TGC	1.84	2.2	3.38	0.07 (n_1=0.122)	0.09 (n_2=0.59)	2.37 (n_3=0.006)	0.10±0.01	2.8±0.2	-
NITGC	1.258	-	3.36	0.02 (n_1=0.32)	-	2.31 (n_2=0.24)	0.15±0.01	-	5.68±0.05

*q_T (J-SA) - Total (J-SA) adsorption capacity

Cu^{2+} ions in high concentration through redistribution of residual surface charges on the carbon matrices. Phase wise adsorbed quantity q (mmol/g) and adsorption efficiency (*n*) are presented in Table 6.

Figure 12 is the John-Sivanandan Achari isotherm plot for H2TGC, where the above much discussed carbon GC is H_2 treated and heated to 950°C. Boehm results exhibit very little phenolic surface functional groups (0.03±0.01). The H_2 treatment has almost entirely cleaned up the surface of GC enough to wash off acidic surface functional groups. But some basic groups exist (0.61±0.01) mol/g. Adsorption of Cu^{2+} ions occurs by cation exchange process results in creating phase I of (H2TGC), (Fig. 12) at low equilibrium concentration. But higher adsorption of q_1 (J) is 0.07 mmol/g, occur in phase I indicates adsorption is favoured by some other hetero atoms on the edges /micro texture of the graphene layers. This means, though phenolic groups of 0.03±0.01 observed, the adsorbed quantity is enhanced by more than twice or generally explained because of extra porosity as evidenced by relatively high BET surface area. More electronegative hetero atoms (than carbon) acquire partial negative charge and thereby, induce partial positive charge on carbon atoms[44]. The Cu^{2+} ions trapped by these surface functional groups may interact laterally with the positively charged carbon surface less favourably. This is marked by the scatter of data plots or the non-uniformity of the isotherm shape in the first phase (H2TGC).

In phase II (H2TGC), the adsorption capacity is found to be (0.09 mmol/g), with adsorbability constant slope $n_2 = 0.59$, In the absence of any free surface functional groups (they are already occupied by Cu^{2+}), indicates significant adsorption probably occurs at the edges of graphene layers which act as the Lewis base centres, operated through π donor-acceptor mechanism.

Phase III (H2TGC), with a very small value of adsorbability constant slope *n* (H2TGC) of 0.006, indicate weak forces of interactions. Adsorption mechanism identical to phase III of carbon (GC) can be expected to occur. Because in H2TGC also, only 2.9% of total adsorption occurs in phase I, 3.8% in phase II and 93.3% occurs in phase III. (Fig. 11).

The John-Sivanandan Achari (J-SA) isotherm plot of NITGC (Fig. 13) is with distinct features of two phases of adsorption. In NITGC, a large number of acidic surface functional groups are produced by the nitric acid treatment. Due to the presence of more
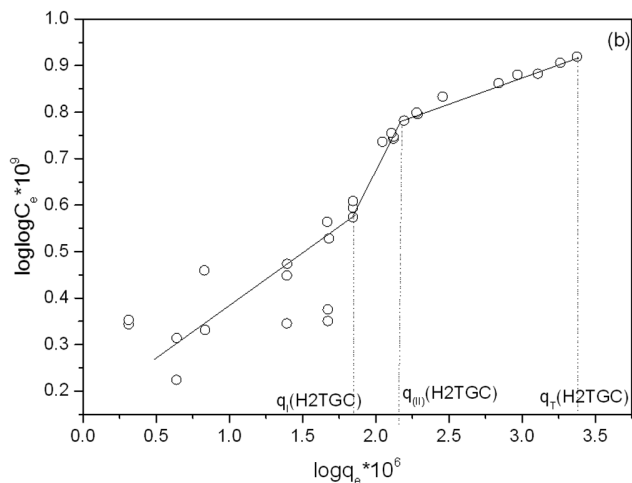
Fig.12 — John-Sivanandan Achari (J-SA) isotherm plots for the adsorption of copper acetate on micro porous carbon (b)H2TGC using equation $loglogC_e=C+nlogq_e$.
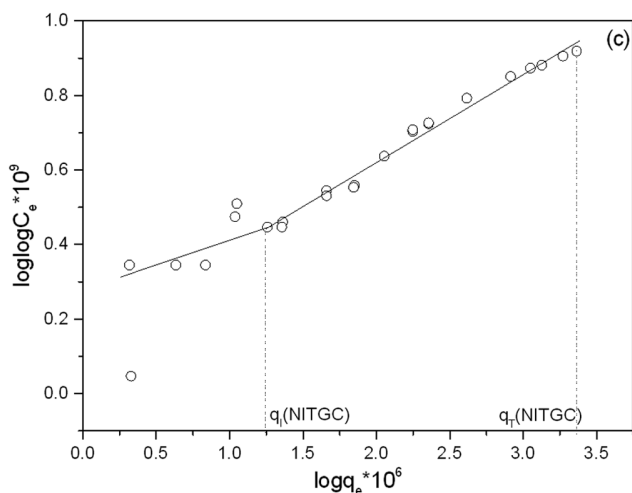
Fig. 13 — John-Sivanandan Achari (J-SA) isotherm plots for the adsorption of copper acetate on micro porous carbon (c) NITGC using equation $loglogC_e=C+ nlogq_e$.

carboxyl groups (1.3 ± 0.1 mmol/g) introduced on the surface, hydrophilicity of the nitric acid treated carbon surface is increased. This leads to the formation of water clusters[47] on the surfaces; may block the creation of an adsorption phase of NITGC analogous to the phase I of the native starting carbon (GC). This leads to missing of the first phase in NITGC compared to H2GC and untreated GC. Afterwards, H^+ ions are adsorbed in preferentially due to their higher ion mobility due to size. This accelerates the uptake of copper hydroxide probably due to hydrogen bonding, to the hydrophilic surface of NITGC. This in turn, favours the increase in solution pH, as more OH accumulates in the medium

cause formation of phase II (NITGC), with a change in adsorption mechanism. Adsorption of Cu^{2+} ions, contributes only 0.02mmol/g to the adsorption in phase 1 of carbon (NITGC).

In phase II (NITGC), higher solution pH favours adsorption of copper hydroxide probably by hydrogen bonding. John-Sivanandan Achari isotherm uptake is found to be 2.31mmol/g for this phase II of carbon NITGC. The BET surface area of carbon GC is decreased from (1560±30) to (1330 ± 30) m^2/g on oxidation of GC using nitric acid that results NITGC. The above discussion follows that the shape of the graph is robustly influenced by the heterogeneity of the carbon surface. The result of regression analysis support this with RSS value of 0.06 for phase I and 0.0062 for phase II as is presented in Table 4. This experimental study[22] adopted a wide concentration range, below 1mmol/g. The smallest concentration selected is (10^{-8} mmol/g). Normally, it requires rigorous mathematical treatments to establish the adsorption mechanism. But the technique of adsorption isotherm analysis deals it rather effortlessly. John-Sivanandan Achari isotherm fitting excellently conforms through these wide ranges of concentrations and provide better inferences on the type of adsorption mechanism, followed based on distinct phases of adsorption resolved on plotting *loglogC_e versus loq q_e*.

Analytically adsorption Phase I is found reserved and related to molecular interactions due to ion exchange mechanism operating in presence of surface functional groups. This involves both acidic and basic groups for GC, but mostly basic functional groups for H2TGC .On the carbon, NITGC large proportion of acidic surface functional groups are introduced during acid treatment. The evaluated John-Sivanandan Achari isotherm adsorbed quantities and the reported Langmuir and Freundlich adsorbed amounts are presented in Table 6. A schematic comparison of adsorbed amount for various isotherm models along with John-Sivanandan Achari isotherm model is given in Fig. 14.

Since a wide range of equilibrium concentrations are used, the reported work adopted a combined form of Langmuir and Freundlich equations[22]. On applying John-Sivanandan Achari isotherm model, the adsorption behaviour of the microporous carbons are satisfactorily evaluated using a single isotherm equation. The isotherm conforms to three phases for GC and H2TGC and only two phases for NITGC
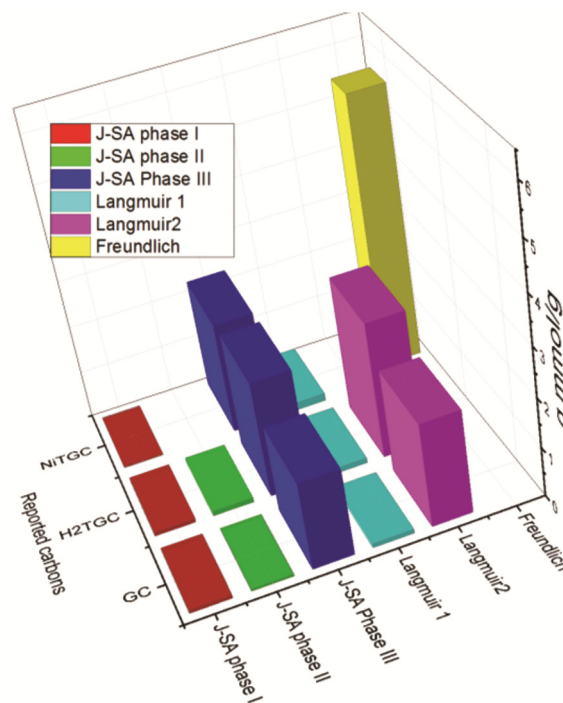
Fig. 14 — Adsorbed quantities obtained for J-SA/Langmuir/ Freundlich isotherm models for the adsorption of Cu^{2+} ions on micro porous carbons

through which the adsorption capacities can be found out, by taking the first inflection point as the *log q(J-SA)* and the highest point as *log q_T(J-SA)* respectively.

IUPAC[34] terminology states that materials with fine pores are called micropores. There are two different types of micropore filling to occur on such materials, just below the initiation of capillary condensation. First is the occupying of individual gas molecules into finer (very narrow) pores, followed by a cooperative process of filling at intermediate pressures due to the interaction of adsorbate molecules. It is required to identify the regions (phases) of micropore filling phenomena once adsorption occur on porous material. This is well differentiated in John and John-Sivanandan Achari isotherm method presented through the above sections and studying both (solid-gas) and (solid-liquid) phenomena. Each phenomenon is identified by distinct features observed. John isotherm method[2] categorises these types of materials as micro porous and 'two lines connects all the experimental points represent the presence of bidisperse pores'. Extrapolation of upper and lower lines respectively give $V_T(J)$ total Limiting Micropore volume (LMV) or $V_f(J)$ (Limiting Micropore Volume of finer pores). Similarly I plots for N_2 gas isotherm give a single and

smooth inversion point as a feature for microporous materials. On applying modified Freundlich method distinct phases are observed identical to John isotherm features exhibited for representative phases for micropore filling. Preferential pore filling mechanism on micro porous carbon has been discussed by earlier researchers[40] supported by the observation made in this study will be useful for the structural characterisation of many of the porous materials involved in the realm of material chemistry.

Conclusion

The study is intended to test the John and John-Sivanandan Achari isotherm model for a micro porous carbon subjected to physical and chemical treatment, for which adsorption from gaseous phase as well as from liquid phase for a wide range of concentration are analysed, keeping the merit of the reported work greatly appreciated.

Applying John isotherm model on published data of carbon GC, H2TGC and NITGC, three phases of adsorption (N_2/77K) are obtained. Phase (I and II) followed by an upper saturation region (phase III) indicate the successive pore filling mechanisms involved in the existing pores. Agreeable results for monolayer with John isotherm model are obtained for most of the isotherm models; Modified Freundlich (F), Langmuir (L), D-R, BET and I plots. NITGC carbon has a high deviation (26.6 %) with John adsorption capacity has highlights many answers. The exact and precise information about the phase changes during adsorption process are accessed rather easily, in the entire range of relative pressure. Visible features of adsorption phases marked by kinks and slopes obtained over the entire concentration region in a direct log-log plot are of the greatest advantage. The results of regression analysis of John isotherm model indicate best fit of the data. As per the categorisation principle reported in the literature as a greatest advantage of John method, the selected carbons are micro porous materials where an activated diffusion and molecular sieve effect leads to phase changes and also place considerable restrictions during pore filling. John isotherm model wisefuly distinguishes them with prominent lines in the graph with adsorption intensity,'n' values (adsorbability constant). Any difference observed between the results of John limiting micropore volume (LMV) or monolayer with respect to the results obtained on applying other isotherm models is due to the phenomena of micropore filling together with pore diffusion effects.

However, in many occasions, the adsorption capacity V (J) and specific surface area SSA (J) by John isotherm method and those calculated by other known isotherm models are in excellent agreement.

Equilibrium isotherm analysis of the adsorption of Cu^{2+} ions on GC, H2TGC and NITGC is not following a single isotherm model for the entire (lower to higher) range of concentrations selected. Adsorption plateu prominent for all carbons at N_2/77K isotherm are missing in liquid phase except of GC. For this carbon too, Langmuir 1 and Langmuir 2 models are required for curve fitting. The rigorous curve fitting exercise using combinations of isotherms leads to inferences. But adsorption efficiency of the material is arguably related to the nature of surface groups given by the respective Boehm tests. The isotherm plots on comparing with John isotherm models for gas and John-Sivanandan Achari isotherm for liquid phase adsorption give prominent phases in the adsorption profile of the Type I isotherm. Adsorption mechanisms are critically described accordingly, for the determination and interpretation of structural parameters of microporous carbons. The results and method of systematic analysis of the adsorption data is most useful for the study of many microporous materials.

References

1   John P T, Suri D K & Nagpal K C, *J Mater Sci, 20* (1985) 2071.
2   John P T & Achari V S, *J Mater Sci,* 37 (2002) 885.
3   Zhang K, Li H, Xu X & Yu H, *Ind Eng Chem Res,* 55 (2016) 2328.
4   Achari V S, *John Isotherm for Liquid Phase Adsorption: Comparison with Langmuir and Freundlich Models*, paper presented at the *International Carbon Conference*, Robert Gordon University, Scotland, UK. 16- 21 July (2006)107.
5   Budinova T, Savova D, Petrov N, Razvigorova M, Minkova V, Ciliz N, Apak E & Ekinci E, *Ind Eng Chem Res*, 42 (2003) 2223.
6   Anitha K, Namsani S & Singh J K, *J Phy Chem A,* 119 (2015) 8349.
7   Achari V S, Jayasree S, & Rajalakshmi A S, *Indian J Chem Technol, 24* (2017) 471.
8   Ismadji S & Bhatia S K, *Can J Chem Eng,* 78 (2000) 892.
9   Subramanyam B & Das A, *J Environ Health Sci & Eng,* 12 (2014) 92.

10 Nouri L & Hamdaoui O, *J. Phy. Chem. A* 111 (2007) 8456.

11 Achari V S, Rajalakshmi A S , Jayasree S and Lopez R M, *Indian Journal of Chemical Technology (accepted, Manuscript No. IJCT 2431)*

12 Xiao B & Thomas K M, *Langmuir* 20 (2004) 4566.

13 Iriarte-Velasco U, Alvarez-Uriarte J I, Chimeno-Alanis N & Gonzalez-Velasco J R,. *Ind. Eng. Chem. Res.* 47 (2008) 7868.

14 Cho H, Wepasnick K, Smith B A, Bangash F K, Fairbrother D H & Ball W P, *Langmuir* , 2 (2010) 967.

15 Carrot P J M, Roberts R A & Sing K S W, *Carbon* 1 (1987) 59.

16 Brunauer S, Emmett P H & Teller E, *J Am Chem Soc*, 60 (1938) 309.

17 Brunauer S, Deming L S, Deming W S & Teller E , *J Am Chem Soc*, 62 (1940) 1723.

18 18 Pomonis P J, Petrakis D E, Ladavos A K, Kolonia K M, Armatas G S, Sklari S D, Dragani P C, Zarlaha A, Stathopoulos V N & Sdoukos A T A, *Mic & Meso Mat,* 69 (2004) 97.

19 Knowles J, Armatas G, Hudson M & Pomonis P, *Langmuir,* 22 (2006) 410.

20 Nagpal K C & John P T, *Carbon,* 16 (1978) 359.

21 John P T , *Ind J Technol,* 26 (1988) 141.

22 Farooq A, Westreich P, Irfan N & Dahn J, *Ind Eng Chem Res,* 48 (2009) 9804.

23 Ajayan P M & Iijima S, *Nature,* 358 (1992) 23.

24 Aa L T J, Achari V S, Rietveld L C, Siegers W G & van Dijk J C, Modeling Biological Activated Carbon Filtration: Determination of Adsorption Isotherms of Organic Compounds. *Proceedings of the 2004 Water Institute of southern Africa Biennial Conference*, Cape Town, 2-6 May (2004)1143.

25 Ringot D, Lerzy B, Chaplain K, Bonhoure J, Auclair E & Larondelle Y, *Bioresour Technol,* 98 (2007) 1812.

26 Chu K H, *Adv Environ Res,* 3 (2014) 131.

27 Jayasree S, Rajalakshmi A S & Achari V S, Determination of Surface Area of Activated Carbons using John-Sivanandan Achari Isotherm Plots, *Proceedings of the 26th Kerala Science Congress*, Pookode, Wayanadu, 28-31 January (2014) 1362.

28 John P T, Suri D K & Nagpal K C, *Carbon,* 20 (1982) 67.

29 John P T, *Indian J Technol,* 27 (1989) 547.

30 Freundlich H, *Z Phys Chem,* Muenchen, Ger. 57(1907) 385.

31 Langmuir I, *J Am Chem Soc.* 38 (1916) 2221.

32 Achari V S, Rajalakshmi A S, Jayasree S & Lopez R M, *J Appl Res Technol, (accepted Nov 2017, Manuscript No JART-D-17-00173)*

33 Dubinin M M, *Chem Rev*, 60 (1960) 235.

34 Thommes M, Kaneko K, Neimark A V, Olivier J P, Rodriguez-Reinoso F, Rouquerol J & Sing K S W. IUPAC Technical Report, *Pure Appl Chem, (*2015) 1.

35 Triantafyllidis K S, Pinnavaia T J, Iosifidis A & Pomonis P J, *J Mater Chem*, 17(2007) 3630.

36 Shahmohammadi-Kalalagh S & Babazadeh H, *Int J Environ Sci Technol*, 11(2014)111.

37 Foo K Y & Hameed B H, *Chem Eng J, 156* (2010) 2.

38 Achari V S & Mercy T, Characterisation of Microporous Materials Using John Isotherm Model paper presented *Proceedings of the 24th Swadeshi Science Congress Organized by Swadeshi Science Movement,* Thunchath Ezhuthachan Malayalam University, Tirur, Malappuram District, Kerala, 6-8 November (2014) 320.

39 Achari V S, Modified Carbons and Wood Dust: Evaluation of Adsorption Properties, *PhD Thesis.* Department of Chemistry, University of Kerala, Thiruvananthapuram - 695581, India, (1998).

40 Song X, Zhang Y, Yan C, Jiang W & Chang C, *J Colloid Interface Sci,* 389 (2013) 213.

41 John P T, Suri D K & Nagpal K C, *Indian J Technol*, 18 (1980) 225.

42 Kaneko K, Ishii C Ruike, M & Kuwabara H, *Carbon,* 1992, 30, 7,1075-1088.

43 Westreich P, Selig S, Fortier H & Dahn J R, *Carbon,* 44 (2006) 3145.

44 Alfarra A, Frackowiak E & Beguin F, *Appl Surf Sci*, 228 (2004) 84.

45 Tumin N D, Chuah A L, Zawani Z & Rashid S A , *J Eng Sci Technol,* 3 (2008) 180.

46 Marsh H & Rodriguez-Reinoso F, *Activated Carbon*, Elsevier Science & Technology Books , ISBN 0080444636 (2006).

47 El-Sheikh A H, *Talanta,* 75 (2008) 127.